Frontiers in Heat and Mass Transfer

Tech Science Press

Doi:10.32604/fhmt.2026.076486

ARTICLE

Spectral Multipole Resonances of Super Elliptic Gold Nanoparticles in the Visible and Near-Infrared Spectral Ranges

Linkang Wang[1], Bowei Xie[2,3,4,*], Zhiqiang Liu[1], Lijing Yi[2,3,4] and Mu Du[2,3,4,*]

[1]Department of Mechanical and Electrical Engineering, Jiangxi Water Resources Institute, Nanchang, 330013, China
[2]Shenzhen Research Institute of Shandong University, Shenzhen, 518000, China
[3]Institute for Advanced Technology, Shandong University, Jinan, 250061, China
[4]Shandong Key Laboratory of Thermal Science and Smart Energy Systems, Shandong University, Jinan, 250061, China

*Corresponding Authors: Bowei Xie. Email: xiebowei@sdu.edu.cn; Mu Du. Email: dumu@sdu.edu.cn

Received: 21 November 2025; Accepted: 30 December 2025; Published: 30 April 2026

ABSTRACT: The Local Surface Plasma Resonance (LSPR) of spherical metal particles is typically only observed within the visible spectrum. This inherent property renders modulation through alterations in radius or material challenging, significantly constraining its practical applications. In this work, we propose a super-elliptic gold nanoparticle model that allows for the continuous modulation of particle geometry from spherical to star-like shapes using a single roundness parameter (e). Unlike conventional nanorods or discrete nanostars, this geometry provides a unified framework to investigate the evolution of multipole resonances. The radiation characteristics of super elliptic gold nanoparticles in the range of 0.3~2.5 μm were calculated by using the Finite Difference Time Domain method. The present study investigates the effects of the particle roundness parameter and particle size on the LSPR response. The results demonstrated that an augmentation in the particle roundness parameter resulted in a substantial enhancement of the absorption efficiency of the particles. Concurrently, a discernible red shift in the LSPR peaks was observed within the visible light spectrum. A greater prevalence of LSPR peaks was observed in the visible and near infrared band for the super elliptical gold nanoparticles with large roundness parameter. Super-elliptical particles have been observed to exhibit multiple plasmonic absorption peaks, in contrast to the more typical behaviour of conventional noble metal particles, which typically exhibit only one or two such peaks. The effect of the roundness parameter on the local surface plasma resonance response of nanoparticles of varying sizes is consistent. The super elliptic gold nanoparticles have potential applications in the fields of solar heating, radiative cooling, biomedical and photocatalysis.

KEYWORDS: Super elliptic; nanoparticles; finite difference time domain method; local surface plasma resonance

1 Introduction

Due to their scale being comparable to that of electromagnetic waves, micro-nano particles exhibit excellent radiation properties and are widely applied in multi-functional coatings, medical care, aerospace, and other fields. Noble metal nanoparticles exhibit unique optical and electrical properties due to the Local Surface Plasma Resonance (LSPR) at specified wavelength [1], which is of great significance in the application of solar heating [2], radiative cooling [3,4], photonic devices [5,6], catalysis [7], biological diagnosis and treatment [8]. The radiative properties of particles are contingent on their composition, geometry, dimensions, and the surrounding medium [9–11]. In the contemporary context, the regulation of the LSPR characteristics of nanoparticles assumes considerable significance in determining the efficacy of their application. In the case of spherical particles, the LSPR peaks are primarily concentrated within the

visible light region. Meanwhile, the range of LSPR characteristics that can be regulated by altering the size of the particles is extremely limited [12,13].

In order to enhance the LSPR intensity of noble metal nanoparticles and modulate the LSPR position, many specific particles have been proposed and have attracted significant attention. In the theoretical study by Zhang et al. [14], plasmonic antennas based on two-step chemically synthesized silver nanoflags constructed by a silver nanowire and a nanoplate were demonstrated. These antennas exhibit high polarization sensitivity and a diversity of spectral signatures dependent on structural parameters arising from observed mode competition. Hong and Wang [15] advanced that negligible modifications to the structural parameters of core-cap nanoparticles will result in a broadband redshift of the LSPR peak within the visible to near-infrared wavelength range. Rodríguez-Oliveros and Sánchez-Gil [16] conducted a theoretical study of the performance of gold nanostars with varying symmetry and tip number as thermal heaters at their corresponding localized surface plasmon resonances. It has been demonstrated that the absorption and scattering cross sections increase with increasing tip number and sharpness of the vertexes. Furthermore, a 30-fold increase of the steady-state temperature is obtained. The objective is to render them suitable for optical heating, and consequently for cancer thermal therapy. Babaei et al. [17,18] proposed a new class of shape-modulated nanoparticles, termed "supershape nanoparticles", through the manipulation of the morphology of a disk-shaped nanoparticle. The results demonstrated the existence of multiple plasmonic modes in these supershape nanoparticles. This study can act as a foundation for the characterisation of multiple particle plasmons in plasmonic devices for sensing applications. As reported by Hashemi et al. [19], the excitation of multiple localized surface plasmons in disk supershape shell nanoparticles was observed. The obtained results demonstrated the presence of two distinct types of plasmon bands, which were found to be dependent on the excitation of dipoles and higher-order multipoles, respectively.

The geometry of the super elliptic particle is defined by the super-ellipsoidal equation, and it evolves from standard spherical particles. As the degree of non-sphericity increases, the particle gradually adopts a spiny morphology, characterized by six sharp spikes [20]. This kind of particle is frequently employed in the modelling of non-spherical aerosol particles in the atmosphere and the study of their radiative properties [21–24]. Nevertheless, the LSPR of super elliptic particles composed of noble metal material remains an area that has not yet been systematically studied. In this study, the radiative characteristics of super gold nanoparticles with radii of 0.01, 0.03, and 0.05 μm in the spectral range from 0.3 to 2.5 μm, are calculated by employing the Finite Difference Time Domain (FDTD) method. The present study investigates the impact of non-spherical degree on the LSPR of particles.

2 Theoretical Parts

2.1 Establishment of the Particle Model

The geometry of the super elliptic particle is delineated by the super-ellipsoidal equation, which is expressed as follows [20,21]:

$$\left[\left(\frac{x}{a}\right)^{2/e}+\left(\frac{y}{b}\right)^{2/e}\right]^{-e/n}+\left[\frac{z}{c}\right]^{2/n}=1 \tag{1}$$

where a, b, and c are three semi-axes along the x, y, and z directions in the Cartesian coordinate system, and e and n are roundness parameters to specify the morphology variation of the particle. The shape of super elliptic particle is spherical shape when $n = e = 1$ and $a = b = c$. In our work, only the condition of $n = e = 1$ and $a = b = c$ is considered. Fig. 1 illustrates the super elliptic particle model with different roundness parameters e, and its potential application in the field of nanofluid and coating is also demonstrated. As illustrated in Fig. 1,

the particle shape transitions from a sphere (e = 1) to an octahedron (e = 2). As the value of e increases, the particle's surfaces gradually become concave, resulting in a spiny particle with six distinct spikes when e equals 3. The super elliptic particles with e ranging from 1 to 3 are sufficient to represent some typical example configurations. For particles with a larger e, it will be difficult to prepare them, and the calculation of their radiation characteristics will be even more challenging to perform accurately. The size parameter of a particle is defined as the ratio of the radius to the wavelength. This ratio is expressed as follows:

$$x = \frac{2\pi r}{\lambda} \tag{2}$$

where λ and r is the incident wavelength and radius, respectively. Due to $r = a = b = c$, it can be deduced that the size parameters for particles exhibiting varying degrees of roundness are equivalent. It is evident that, for particles exhibiting equivalent size parameters, an augmentation in the roundness parameter is concomitant with a diminution in volume. This phenomenon can be attributed to the spiny configuration of the particles, which is characterized by six distinct spikes.

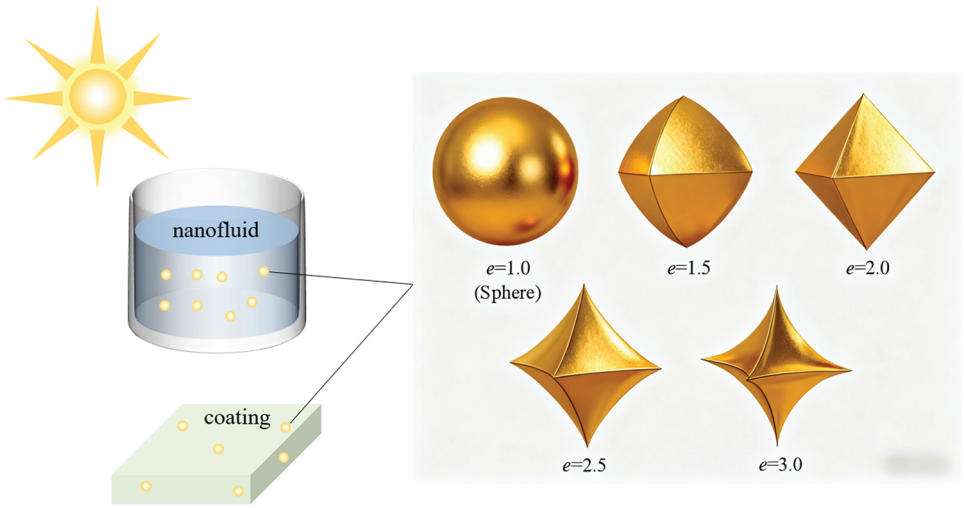

Figure 1: Diagram of super elliptic particle model

2.2 Calculation Method

The absorption cross section C_{abs} is defined as the ratio of the sum of the electromagnetic energy absorbed by the particle to the energy of the incident electromagnetic wave. In a similar manner, the scattering cross section, denoted C_{sca}, is defined as the ratio of the sum of the electromagnetic energy scattered by the particle to the energy of the incident electromagnetic wave. The absorption efficiency Q_{abs} and scattering efficiency Q_{sca} is defined as:

$$Q_{abs} = \frac{C_{abs}}{\pi {r_e}^2} \tag{3}$$

$$Q_{sca} = \frac{C_{sca}}{\pi {r_e}^2} \tag{4}$$

where r_e is the radius of equivalent volume sphere of the super elliptic particle. The equivalent solar absorption efficiency $Q_{abs,solar}$ and average absorption efficiency $Q_{abs,ave}$ are defined as:

$$Q_{abs,solar} = \frac{\int_{0.3\mu m}^{2.5\mu m} S_\lambda C_{abs} d\lambda}{S\pi r^2} \tag{5}$$

$$Q_{abs,ave} = \frac{\int_{0.3\mu m}^{2.5\mu m} C_{abs} d\lambda}{\pi r^2 \int_{0.3\mu m}^{2.5\mu m} d\lambda} \tag{6}$$

where the S is the solar constant, i.e., 1422 W/m^2, and S_λ is the solar spectral radiation density.

In this study, the super elliptic particle under investigation is composed of Au, and the complex refractive index m of Au is illustrated in Fig. 2a [25]. Fig. 2b presents the spectral absorption efficiency cloud map of spherical gold nanoparticles with different radii. Plasmonic behavior is typically observed under conditions where the particle size is relatively small. As demonstrated in Fig. 2b, particles with a diameter ranging from 0.01 to 0.05 μm encompass the spectrum where the absorption peak occurs. Consequently, particles with radius of 0.05, 0.03, and 0.01 μm were selected as the research object and the radiation characteristics were calculated using the FDTD method. In FDTD, the mesh sizes are set to be less than 0.5 nm. The incident light is characterized as parallel incident light, with the incident direction aligning along the semi-axis of the super elliptic Au particle. The accuracy of the model is verified by the Mie theory. Fig. 3 illustrates the absorption efficiency and scattering efficiency of spherical Au particle calculated by the FDTD method and the Mie theory. As demonstrated in Fig. 3, when the mesh size is set at 0.5 nm, the FDTD method is capable of accurately calculating the absorption and scattering efficiency of spherical particles within the wavelength range of 0.3 to 2.5 μm. Consequently, the mesh size of 0.5 nm is sufficiently small to ensure the attainment of precise results by FDTD method.

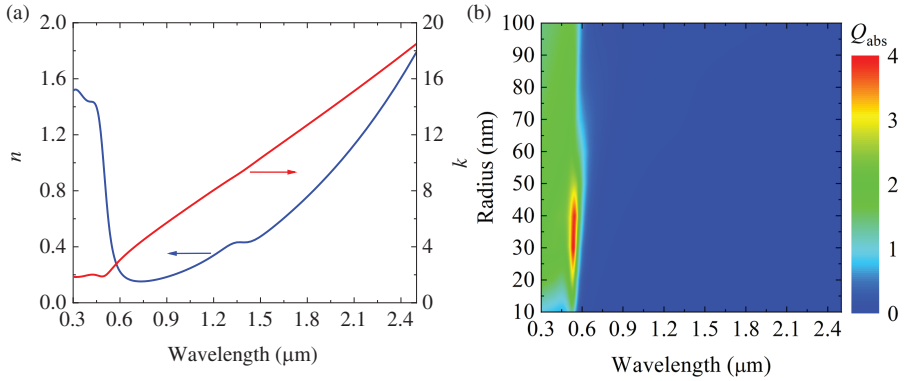

Figure 2: (**a**) The complex refractive index of gold m [25]. (**b**) The spectral absorption efficiency cloud map of spherical gold nanoparticles with different radii

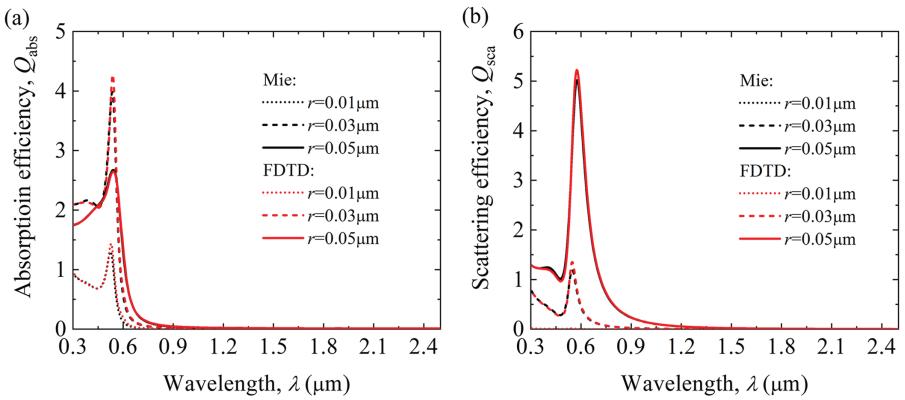

Figure 3: The comparison diagram of (**a**) absorption efficiency and (**b**) scattering efficiency of spherical particles calculated by FDTD method and Mie theory [26] when the mesh size is 0.5 nm

3 Result and Analysis

Fig. 4 illustrates the absorption efficiency and the absorption cross section of super elliptic Au particles with different roundness parameter *e* and particle radius *r*. The figure illustrates that, as the ellipticity parameter of the super-elliptical particle increases from 1 to 2, that is, as the particle changes from a spherical shape to a standard hexahedron, the absorption peak of the particle remains in the visible light region. A notable increase in the peak of the particle absorption efficiency, accompanied by a discernible trend of red shift, can be attributed to the pronounced corners of the standard hexahedron shape, which would largely enhance the LSPR. This observation is consistent with the research findings of Rodríguez-Oliveros et al. [16]. As the ellipticity parameter of the super-elliptical particle continues to increase from 2 to 3, in addition to the peak in the visible light region, an obvious absorption peak appears in the near-infrared region, and the number of absorption peaks also increases to 5.

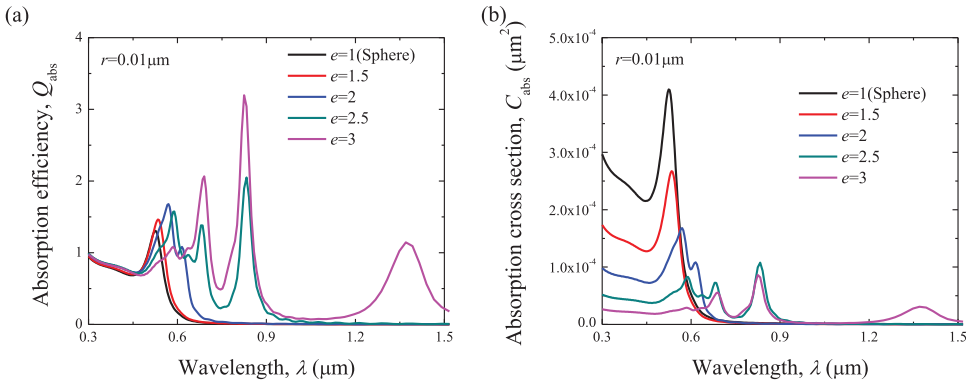

Figure 4: (Continued)

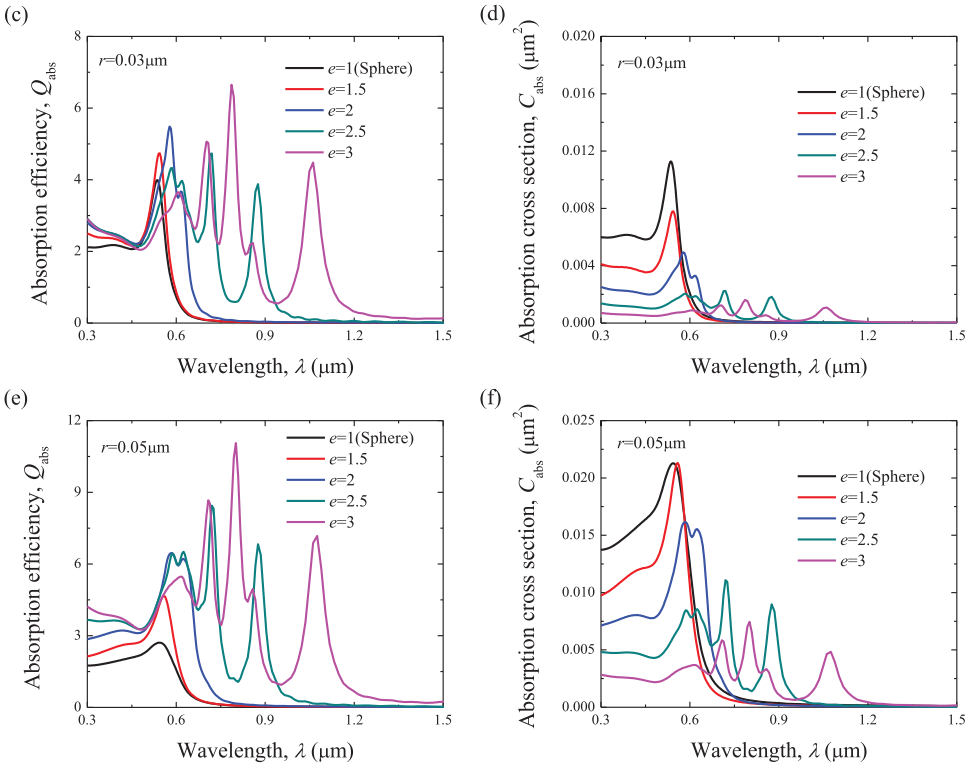

Figure 4: The (**a**,**c**,**e**) absorption efficiency and (**b**,**d**,**f**) the absorption cross section of super elliptic Au particles with different roundness parameter *e* and particle radius *r*

As illustrated in Fig. 4b,e, the particle absorption ability exhibited an increasing trend with the rise in the roundness parameter, when the particle radius increased from 0.01 to 0.03 and 0.05 μm. Furthermore, the presence of multiple absorption peaks was also evident. It is noteworthy that when the particle radius is 0.01 μm, the increase of the roundness parameter primarily leads to an augmentation in the number and magnitude of the absorption peaks in the near-infrared band. However, when the particle radius increases to 0.05 μm, the spectral absorption efficiency increases with the increase of the roundness parameter in the entire solar band. Concurrently, the particle radius exerts a substantial influence on the position of the absorption peak.

Furthermore, an inverse relationship is observed between the absorption cross section of super-elliptical particles and the roundness parameter, with the latter increasing, resulting in a decrease in the former. The primary reason for this phenomenon is that, as the roundness parameter, e, increases, the volume of the particles gradually decreases. Concurrently, the absorption efficiency of the particles shows a significant increasing trend with the increase of the roundness parameter. It can thus be concluded that super-elliptical particles with a larger roundness parameter exhibit a stronger light absorption ability.

Fig. 5 shows the curve of the number of absorption peaks of super-elliptical particles with different particle radii changing with the roundness parameter. As demonstrated in Fig. 5, for super-elliptical particles with varying radii, the number of absorption peaks increases monotonically with an increase in the roundness parameter *e*. Furthermore, the number of absorption peaks of particles with different radii under the same roundness parameter remains consistent. Consequently, the number of absorption peaks exhibited by super-elliptical particles is not contingent on the particle radius; instead, it is predominantly influenced by the roundness parameter of the particles.

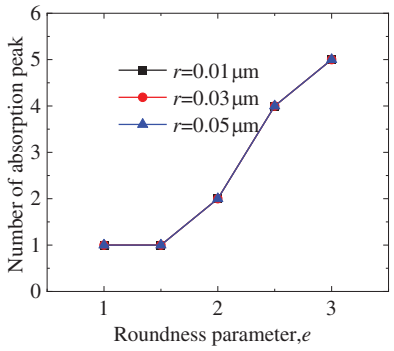

Figure 5: The number of absorption peaks of super ellipse particles with the roundness parameter *e* at different particle radius *r*

Taking the utilization of solar energy as an example, we calculated the equivalent solar absorption efficiency, and the results are shown in Fig. 6. Concurrently, the mean absorption efficiency is exhibited in Fig. 6. As demonstrated in Fig. 6, the equivalent solar absorption efficiency remains almost unchanged for particles with a diameter of 0.01 μm as the roundness parameter increases. This phenomenon can be attributed to the fact that, when the particle size is set to 0.01 μm and the roundness parameter is increased, the enhancement of the spectral absorption efficiency of the particles is predominantly observed within the near-infrared spectral range. Furthermore, the distribution of solar radiation in the near-infrared spectral range is comparatively reduced relative to the visible light band. For particles with diameters of 0.03 and 0.05 μm, the equivalent solar absorption efficiency increases significantly as the roundness parameter increases. Furthermore, it has been demonstrated that the average absorption cross section increases monotonically with an increase in the roundness parameter. Consequently, super ellipse particles have considerable application prospects in the field of solar energy utilization. The overall absorption characteristics of super-elliptical particles are found to be predominantly influenced by *e*, exhibiting a consistent influence on the absorption characteristics of particles across various sizes. This finding aligns with the conclusions of numerous extant studies [27–29], which demonstrate that particle absorption is significantly influenced by their shape, while within a certain range, the impact of particle size is constrained.

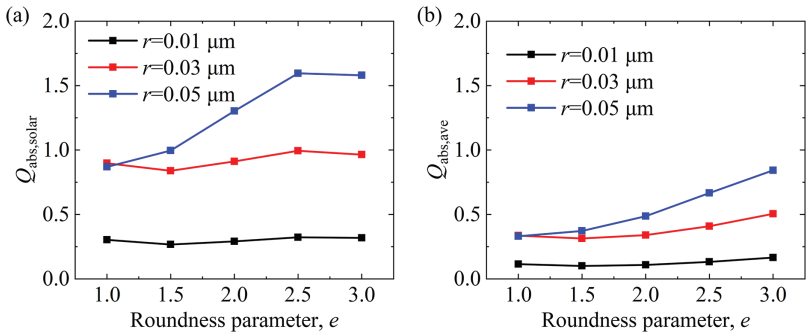

Figure 6: The (**a**) equivalent solar absorption efficiency and (**b**) average absorption efficiency of super ellipse particles as a function of the roundness parameter *e* for different particle radius *r*

In addition to the absorption property, the scattering property of particles has a significant impact on the radiative transfer characteristics of the particle group and affects the practical application effect. It is widely accepted that particle scattering constitutes the primary mechanism by which electromagnetic radiation undergoes a change in its propagation direction upon encountering minute particles during transmission

through a medium. The redistribution of radiation energy direction is a key factor in the significant effect on the radiation transmission process. The precise description of particle scattering properties is crucial for radiation transmission calculations and inversions. Fig. 7 illustrates (a,c,e) the scattering efficiency and (b,d,f) the scattering cross section of super elliptic Au particles with different roundness parameters and particle radius. As demonstrated in Fig. 7, in contrast to the absorption characteristics of the particles, as the roundness parameter of the super elliptic particles increases, the particle scattering efficiency monotonically decreases. This phenomenon can be attributed to the fact that as the roundness parameter increases, the actual volume of the particles decreases and their scattering ability is reduced. Simultaneously, as the roundness parameter of the particles is increased, there is no significant shift in the position of the scattering peak and the number of scattering peaks does not increase significantly. Furthermore, for super elliptic particles of varying diameters, the trend of the particle scattering characteristics with respect to the roundness parameter is essentially equivalent.

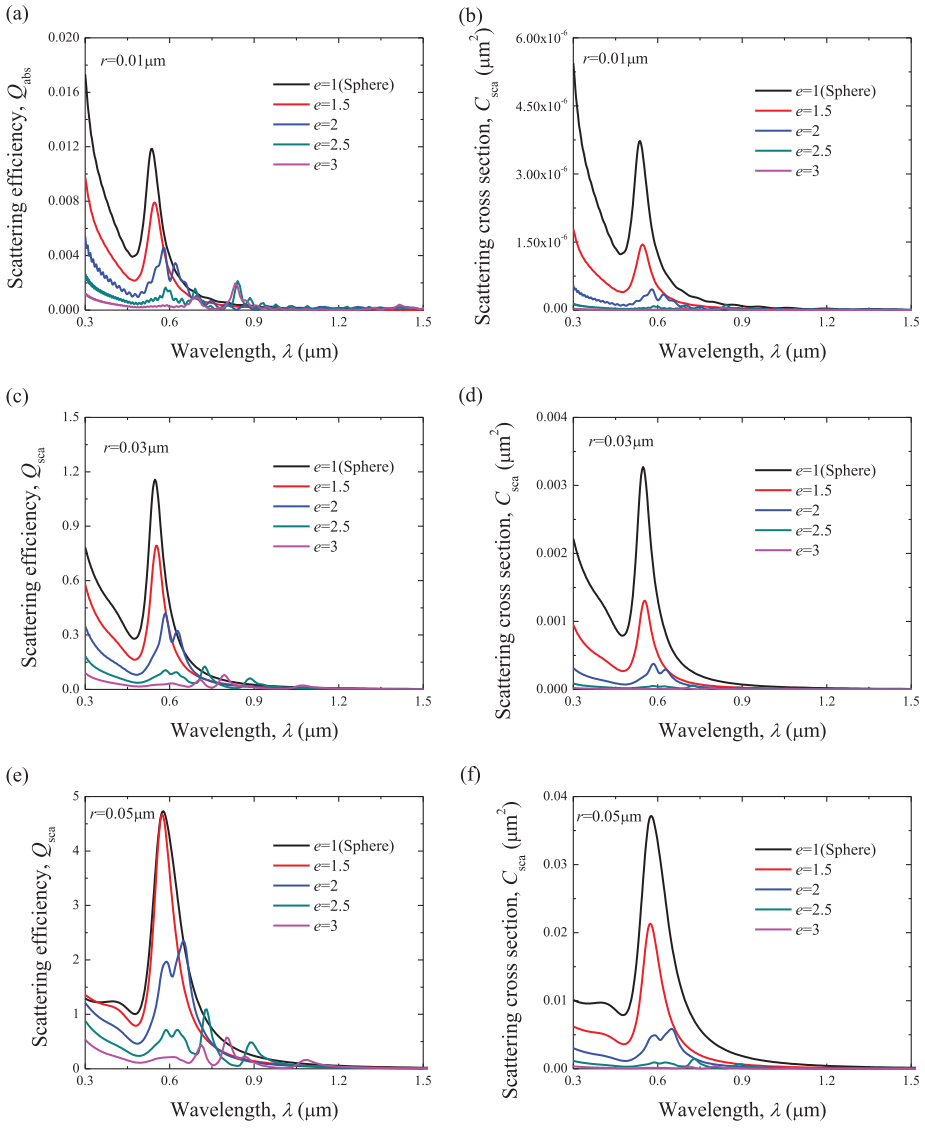

Figure 7: The (**a**,**c**,**e**) scattering efficiency and (**b**,**d**,**f**) the scattering cross section of super elliptic particles at different roundness parameters *e* and particle radius *r*

This outstanding absorption performance of the super-elliptical particles gives it great potential for application in the fields of solar heating, radiative cooling, biomedical and photocatalysis. Super-elliptical particles have been shown to exhibit superior absorption properties, particularly with regard to the manifestation of multiple absorption peaks within the near-infrared range. They can be combined with nanofluids or coatings to enhance the solar absorption efficiency [28,29]. Furthermore, the LSPR characteristics of super-elliptical particles have the potential to enable their combination with radiation cooling coatings, thereby generating specific structural colors and enhancing the aesthetic appeal of the coatings. In the field of photocatalysis, particles that exhibit superior LSPR properties have been shown to enhance the catalytic efficiency of the system by increasing light absorption [27]. In the domain of biomedicine, the pronounced anisotropic absorption properties of such particles result in the generation of localized high temperatures, thereby facilitating the destruction of diseased cells.

4 Conclusion

The radiative characteristics of super elliptic gold nanoparticles in the wavelength range from 0.3 to 2.5 μm are calculated by employing the FDTD method. The present study investigates the effects of the particle roundness parameter and particle size on the LSPR response. The results demonstrated that an increase in the particle roundness parameter resulted in a substantial enhancement in the absorption efficiency of the particle. Concurrently, the LSPR peak in the visible light band exhibited a pronounced red shift. It is evident that the number of LSPR peaks of the particle would increase in proportion to the increase of the roundness parameter. In the case of super-elliptical gold nanoparticles with $e = 3$, five distinct LSPR peaks were observed in the visible near-infrared region, with the strongest peak located at a wavelength equal to 1 μm. The influence law of the roundness parameter e on the localized surface plasmon resonance response of nanoparticles of different sizes was consistent. It is evident that super-elliptical gold nanoparticles, due to their unique LSPR characteristics, have considerable potential for application in a variety of fields, including solar heating, radiative cooling, biomedical and photocatalysis.

Acknowledgement: The scientific calculations in this paper have been done on the HPC Cloud Platform of Shandong University.

Funding Statement: This work was supported by the Science and Technology Research Project of Department of Education of Jiangxi Province (GJJ2409205), and Basic and Applied Basic Research Foundation of Guangdong Province (2024A1515011867, 2024A1515011379, 2023A1515110613).

Author Contributions: The authors confirm contribution to the paper as follows: Conceptualization, Bowei Xie; methodology, Linkang Wang and Bowei Xie; software, Linkang Wang and Bowei Xie; validation, Linkang Wang and Bowei Xie; formal analysis, Linkang Wang, Lijing Yi and Zhiqiang Liu; investigation, Linkang Wang and Zhiqiang Liu; resources, Bowei Xie; data curation, Linkang Wang and Zhiqiang Liu; writing—original draft preparation, Linkang Wang; writing—review and editing, Bowei Xie and Mu Du; visualization, Linkang Wang and Bowei Xie; supervision, Mu Du; project administration, Bowei Xie; funding acquisition, Bowei Xie and Mu Du. All authors reviewed the results and approved the final version of the manuscript.

Availability of Data and Materials: The data that support the findings of this study are available from the Corresponding Author, Mu Du, upon reasonable request.

Ethics Approval: Not applicable.

Conflicts of Interest: The authors declare no conflicts of interest to report regarding the present study.

References

1. Petryayeva E, Krull UJ. Localized surface plasmon resonance: nanostructures, bioassays and biosensing—a review. Anal Chim Acta. 2011;706(1):8–24. doi:10.1016/j.aca.2011.08.020.
2. Wang X, He Y, Chen M, Hu Y. ZnO-Au composite hierarchical particles dispersed oil-based nanofluids for direct absorption solar collectors. Sol Energy Mater Sol Cells. 2018;179:185–93. doi:10.1016/j.solmat.2017.11.012.
3. Zhao X, Li T, Xie H, Liu H, Wang L, Qu Y, et al. A solution-processed radiative cooling glass. Science. 2023;382(6671):684–91. doi:10.1126/science.adi2224.
4. So S, Yun J, Ko B, Lee D, Kim M, Noh J, et al. Radiative cooling for energy sustainability: from fundamentals to fabrication methods toward commercialization. Adv Sci. 2024;11(2):2305067. doi:10.1002/advs.202305067.
5. Sorger VJ, Zhang X. Spotlight on plasmon lasers. Science. 2011;333(6043):709–10. doi:10.1126/science.1204862.
6. Xiao J, Yin K, Wang L, Pei J, Song X, Huang Y, et al. Femtosecond laser atomic-nano-micro fabrication of biomimetic perovskite quantum dots films toward durable multicolor display. ACS Nano. 2025;19(25):23431–41. doi:10.1021/acsnano.5c06945.
7. Hartland GV, Besteiro LV, Johns P, Govorov AO. What's so hot about electrons in metal nanoparticles? ACS Energy Lett. 2017;2(7):1641–53. doi:10.1021/acsenergylett.7b00333.
8. Pissuwan D, Valenzuela SM, Cortie MB. Therapeutic possibilities of plasmonically heated gold nanoparticles. Trends Biotechnol. 2006;24(2):62–7. doi:10.1016/j.tibtech.2005.12.004.
9. Mishchenko MI, Lacis AA, Travis LD. Scattering, absorption, and emission of light by small particles. Cambridge, UK: Cambridge University Press; 2002.
10. Xie BW, Ma LX, Zhao JM, Liu LH, Wang XZ, He YR. Experimental study of the radiative properties of hedgehog-like ZnO-Au composite particles. J Quant Spectrosc Radiat Transf. 2019;232(7536):93–103. doi:10.1016/j.jqsrt.2019.05.006.
11. Xie B, Dong J, Zhao J, Liu L, Fu X, Zhai Z. VO_2 particle-based intelligent metasurface with perfect infrared emission for the spacecraft thermal control. Appl Opt. 2022;61(35):10538–47. doi:10.1364/AO.475672.
12. Xie B, Ma L, Zhao J, Liu L. Dependent absorption property of nanoparticle clusters: an investigation of the competing effects in the near field. Opt Express. 2019;27(8):A280–91. doi:10.1364/OE.27.00A280.
13. Halas N. Playing with plasmons: tuning the optical resonant properties of metallic nanoshells. MRS Bull. 2005;30(5):362–7. doi:10.1557/mrs2005.99.
14. Zhang XY, Zhang T, Hu A, Song YJ, Duley WW. Controllable plasmonic antennas with ultra narrow bandwidth based on silver nano-flags. Appl Phys Lett. 2012;101(15):153118. doi:10.1063/1.4759122.
15. Hong X, Wang C. Optical properties of single core-capped nanoparticles. Acta Opt Sin. 2018;38(5):0524001. doi:10.3788/aos201838.0524001.
16. Rodríguez-Oliveros R, Sánchez-Gil JA. Gold nanostars as thermoplasmonic nanoparticles for optical heating. Opt Express. 2012;20(1):621–6. doi:10.1364/OE.20.000621.
17. Babaei F, Javidnasab M, Rezaei A. Supershape nanoparticle plasmons. Plasmonics. 2018;13(4):1491–7. doi:10.1007/s11468-017-0655-5.
18. Babaei F, Javidnasab M, Rezaei A. Localized surface plasmons of supershape nanoparticle dimers. Plasmonics. 2019;14(2):285–91. doi:10.1007/s11468-018-0803-6.
19. Hashemi P, Yaghooti E, Babaei F. Localized surface plasmons in disk supershape shell nanoparticles. J Opt Soc Am B. 2025;42(6):1366. doi:10.1364/josab.559793.
20. Faux ID, Pratt MJ. Computational geometry for design and manufacture. Chichester, UK: Ellis Horwood Ltd.; 1979.
21. Bi L, Lin W, Liu D, Zhang K. Assessing the depolarization capabilities of nonspherical particles in a super-ellipsoidal shape space. Opt Express. 2018;26(2):1726–42. doi:10.1364/OE.26.001726.
22. Xi Y, Bi L, Lin W. Application of deep learning to enhance the computation of phase matrices of nonspherical atmospheric particles across all size parameters. J Geophys Res Mach Learn Comput. 2025;2(3):1–22. doi:10.1029/2025JH000628.

23. Wang X, Bi L, Wang H, Wang Y, Han W, Shen X, et al. AI-NAOS: an AI-based nonspherical aerosol optical scheme for the chemical weather model GRAPES_Meso5.1/CUACE. Geosci Model Dev. 2025;18(1):117–39. doi:10.5194/gmd-18-117-2025.
24. Bi L, Wang Z, Han W, Li W, Zhang X. Computation of optical properties of core-shell super-spheroids using a GPU implementation of the invariant imbedding T-matrix method. Front Remote Sens. 2022;3:903312. doi:10.3389/frsen.2022.903312.
25. Johnson PB, Christy RW. Optical constants of the noble metals. Phys Rev B. 1972;6(12):4370–9. doi:10.1103/physrevb.6.4370.
26. Bohren CF, Huffman DR. Absorption and scattering of light by small particles. Hoboken, NJ, USA: John Wiley & Sons, Inc.; 1998. doi:10.1002/9783527618156.
27. Xie BW, Dong J, Zhao JM, Liu LH. Radiative properties of hedgehog-like ZnO-Au composite particles with applications to photocatalysis. J Quant Spectrosc Radiat Transf. 2018;217:1–12. doi:10.1016/j.jqsrt.2018.04.036.
28. Du M, Tang GH. Plasmonic nanofluids based on gold nanorods/nanoellipsoids/nanosheets for solar energy harvesting. Sol Energy. 2016;137(11):393–400. doi:10.1016/j.solener.2016.08.029.
29. Yu X, Huang M, Wang X, Sun Q, Tang GH, Du M. Toward optical selectivity aerogels by plasmonic nanoparticles doping. Renew Energy. 2022;190:741–51. doi:10.1016/j.renene.2022.03.102.